ELSEVIER

Contents lists available at ScienceDirect

Journal of Molecular Spectroscopy

journal homepage: www.elsevier.com/locate/yjmsp





The 130 – 750 GHz rotational spectrum of 2-cyanopyridine – Analysis of the ground vibrational state and the Coriolis-coupled dyad of its lowest-energy fundamental states

P. Matisha Dorman, Brian J. Esselman, Maria A. Zdanovskaia, R. Claude Woods *, Robert J. McMahon *

Department of Chemistry, University of Wisconsin-Madison, 1101 University Avenue, Madison, WI 53706, USA

ABSTRACT

The millimeter-wave rotational spectrum of 2-cyanopyridine was collected from 130 to 750 GHz, and the ground and two lowest-energy excited vibrational states were analyzed. In total, over 20,000 rotational transitions were least-squares fit for the three vibrational states to partial-octic, distorted-rotor Hamiltonians with low error (σ_{fit} < 50 kHz). For the ground state, the many thousands of newly measured rotational transitions enabled substantial refinement of the rotational constants and determination of the centrifugal distortion constants. The rotational spectrum was collected at room temperature, permitting the observation of the two lowest-energy fundamental modes, ν_{30} (A', 154 cm⁻¹) and ν_{21} (A', 175 cm⁻¹), and determination of their spectroscopic constants. The two excited vibrational states are Coriolis coupled and require a two-state Hamiltonian. Eight Coriolis-coupling parameters (G_a , G_a^I , G_a^K , G_a^I , F_{bc} , F_{bc} , G_b , and G_b^I) have been determined, as well as a precise energy difference of 26.524 312 6 (40) cm⁻¹ between the vibrational states. A comparison of the ground-state spectroscopic constants, as well as the Coriolis coupling-related parameters of analogous dyads is presented for multiple cyanoarenes.

1. Introduction

The cyanopyridine isomers [1,2] and other cyano-substituted arenes [3-5] have become of particular interest to our group following the recent detections of several substituted, five- and six-membered ringcontaining aromatic molecules in the interstellar medium (ISM): benzonitrile [6], cyanoindenes [7] and cyanonaphthalenes [8]. The detection of these aromatic nitriles in the interstellar medium provides strong evidence for the presence of their parent aromatic species. Benzene was initially detected in the ISM via infrared spectroscopy [9], but cannot be observed with radioastronomy because it lacks a permanent dipole moment. The CN substitution of the benzene ring in benzonitrile provides a permanent dipole moment that, combined with its abundance in the source (TMC-1), enabled its detection by rotational spectroscopy. Pyridine, the N-heterocyclic analogue of benzene, has a moderate permanent dipole moment of 2.2 D, but has so far eluded detection in the ISM [10-13]. There are three regioisomeric nitrile-substituted pyridines (Fig. 1), two of which (2- and 3-cyanopyridine) have substantially larger dipole moments than pyridine, and all are attractive candidates for radioastronomical detection [14].

Recently, our group has analyzed the spectra of 3-cyanopyridine [1] and 4-cyanopyridine [2], and greatly expanded the number of reported rotational transition frequencies in their ground and two lowest-energy vibrationally excited states. The ground vibrational state of both of these isomers is adequately modeled by a distorted-rotor Hamiltonian, while the lowest-energy excited vibrational states exhibit Coriolis coupling, complicating the analysis of their rotational spectra. Quartic and sextic distortion constants, Coriolis perturbation terms, and a precise energy separation for the dyad of vibrational states were determined by applying a multi-state model. These reported transition frequencies and spectroscopic constants, combined with those from previous works, provide the foundation of future radioastronomical searches. As with the earlier studies on 3- and 4-cyanopyridine, the current work on 2-cyanopyridine greatly expands the list of assigned rotational transition frequencies and provides spectroscopic constants for the ground and two lowest-energy vibrationally excited states.

2-Cyanopyridine (Fig. 2) is a G_5 , near-prolate ($\kappa = -0.850$), asymmetric rotor with the largest measured dipole moment of the three cyanopyridine isomers ($\mu_a = 5.47$ (10) D and $\mu_b = 1.87$ (3) D, [14]). Recently, Vogt et al. utilized the previous microwave data and vibrational frequency measurements, along with new gas-phase electron diffraction spectroscopy, to determine an equilibrium structure for each of the cyanopyridine regioisomers [15–17]. The only reported rotational transitions for 2-cyanopyridine, however, are 22 transitions between 8

E-mail addresses: rcwoods@wisc.edu (R.C. Woods), robert.mcmahon@wisc.edu (R.J. McMahon).

^{*} Corresponding authors.

$$C \equiv N$$
 $C \equiv N$ $C \equiv$

Fig. 1. 2-, 3-, and 4-Cyanopyridine regioisomers with experimental dipole moments [14].

and 17 GHz [18]. Although no quadrupole splitting was observed, the observation of intense a- and b-type rotational transitions provided adequate determination of the A_0 , B_0 , and C_0 rotational constants. Fundamental vibrational frequencies via infrared and Raman spectroscopy of all of the cyanopyridine isomers have been reported, including those of v_{30} (A'', 154 cm⁻¹) and v_{21} (A', 175 cm⁻¹) for 2-cyanopyridine [19].

2. Experimental and computational methods

A commercially available sample of 2-cyanopyridine was used without purification. The millimeter-wave spectrometer has been previously described, and the frequency range has recently been expanded to 750 GHz [20-22]. Spectral segments from 130 - 235 GHz, 235 - 360 GHz, 365 - 500 GHz, and 500 - 750 GHz were collected at room temperature and combined into a single spectrum using Kisiel's Assignment and Analysis of Broadband Spectra software [23,24]. The rotational spectra were collected at a sample pressure of 5 mTorr in a continuous flow in order to maintain a pure sample and constant pressure throughout data collection. The complete spectrum from 130 to 750 GHz was obtained using automated data collection software over approximately twelve days with these experimental parameters: 0.6 MHz/sec sweep rate, 10 ms time constant, and 50 kHz AM and 500 kHz FM modulation in a tone-burst design [25]. Pickett's SPFIT/SPCAT [26] was used for least-squares fitting, and analyses were completed using PIFORM, PLANM, and AC [27,28]. A measurement uncertainty of 50 kHz was used for all newly acquired frequencies, and the specified measurement uncertainty of 200 kHz was used for transitions reported by Doraiswamy and Sharma [18].

The optimized molecular geometry of 2-cyanopyridine was obtained using very tight convergence criteria with an ultrafine integration grid (opt = verytight and int = grid = ultrafine). Computations were performed at the B3LYP/6-311+G(2d,p) level of theory using Gaussian 16 through the WebMO interface [29,30]. Predicted values of the fundamental vibrational frequencies, spectroscopic constants, vibration-rotation interaction constants, Coriolis coupling constants (ζ), and quartic and sextic centrifugal distortion constants were determined from an anharmonic frequency calculation. Computational output files are provided in the supplementary material.

3. 2-Cyanopyridine rotational spectra

The rotational spectrum of 2-cyanopyridine is similar to those of structurally analogous molecules 2-cyanopyrimidine [4], cyanopyrazine [5], 3-cyanopyridine [1], 4-cyanopyridine [2], phenyl isocyanide [31], benzonitrile [32,33], 2-furonitrile [3], and phenylacetylene [34]. As shown in Fig. 3, despite this molecule being a prolate top, the most visually apparent features of the spectrum of 2-cyanopyridine are oblate-type bands of intense a-type R-branch transitions, at least up to approximately 400 GHz. Above that frequency (Fig. 4), the inherently weaker b-type R-branch transitions begin to dominate the spectrum. Many weaker Q-branch, but no P-branch, transitions were observed. As with the analogous molecules, transitions arising from many

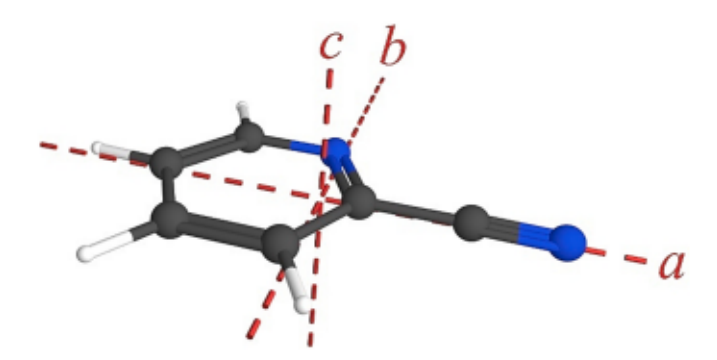


Fig. 2. 2-Cyanopyridine (C_s , $\mu_a = 5.47$ D and $\mu_b = 1.87$ D [14]) in the principal inertial axis system.

vibrationally excited states are apparent in the spectrum (Fig. 3), but only those from the two lowest-energy fundamental states were analyzed in this work.

3.1. Ground vibrational state

The observed frequency range for 2-cyanopyridine, namely 130 -750 GHz, provided a large number of ground-state transitions (Fig. 5). The vast majority of the measured transitions have frequencies below 500 GHz, since only the most intense transitions beyond 500 GHz could be measured, mainly due to hardware limitations. A total of 10,606 distinct transitions were measured and least-squares fit to a partial-octic, distorted-rotor Hamiltonian (Gfit = 40 kHz). The previously reported rotational constants [18] and predicted quartic and sextic distortion constants were used to initially identify the most intense K_a series of the ground vibrational state, then refined with additional data. In the data distribution plots shown in Fig. 5, the range of new millimeter-wave transitions for the ground vibrational state appears in black, and the incorporated microwave transitions from Doraiswamy and Sharma [18] are presented in blue. The final data set includes transitions ranging in J'values from 2 to 195 and with K_a'' values from 0 to 66. The wide frequency range, variety of transition types, extensive J/K quantum number range, and the very large number of transitions in the final data set allowed for an excellent determination of a partial-octic, centrifugally distorted Hamiltonian in both the A and S reductions using the If representation.

The 2-cyanopyridine spectroscopic constants are presented in Table 1 in both the S and A reductions using the I representation. In both reductions, the data set did not permit the determination of a complete set of octic centrifugal distortion constants. The previously reported C₀ value, 1254.460 (4) MHz [18], is in good agreement with the value determined in the present work. In contrast, the values of A0 and Bo (5836.756 (14) MHz and 1598.219 (4) MHz, respectively) are not in agreement with the more accurate and precise values from the current work. The newly determined values are improved by the addition of over 10,500 new rotational transitions and the successful incorporation of many new centrifugal distortion terms into the Hamiltonian. The inertial defect of the ground state, $\Delta_i = 0.073069$ (6) uÅ², is consistent with a planar molecule. All of the quartic and sextic distortion constants could be satisfactorily determined. The value of the h1 constant, however, is of some concern because the magnitude is very small (and only four times greater than its statistical uncertainty) and the sign is opposite that of its B3LYP-predicted value. The value of h_1 is predicted to be quite small relative to the other centrifugal distortion constants, so the discrepancy between predicted and observed values could be caused by a quite small absolute error in the computed value. The experimental

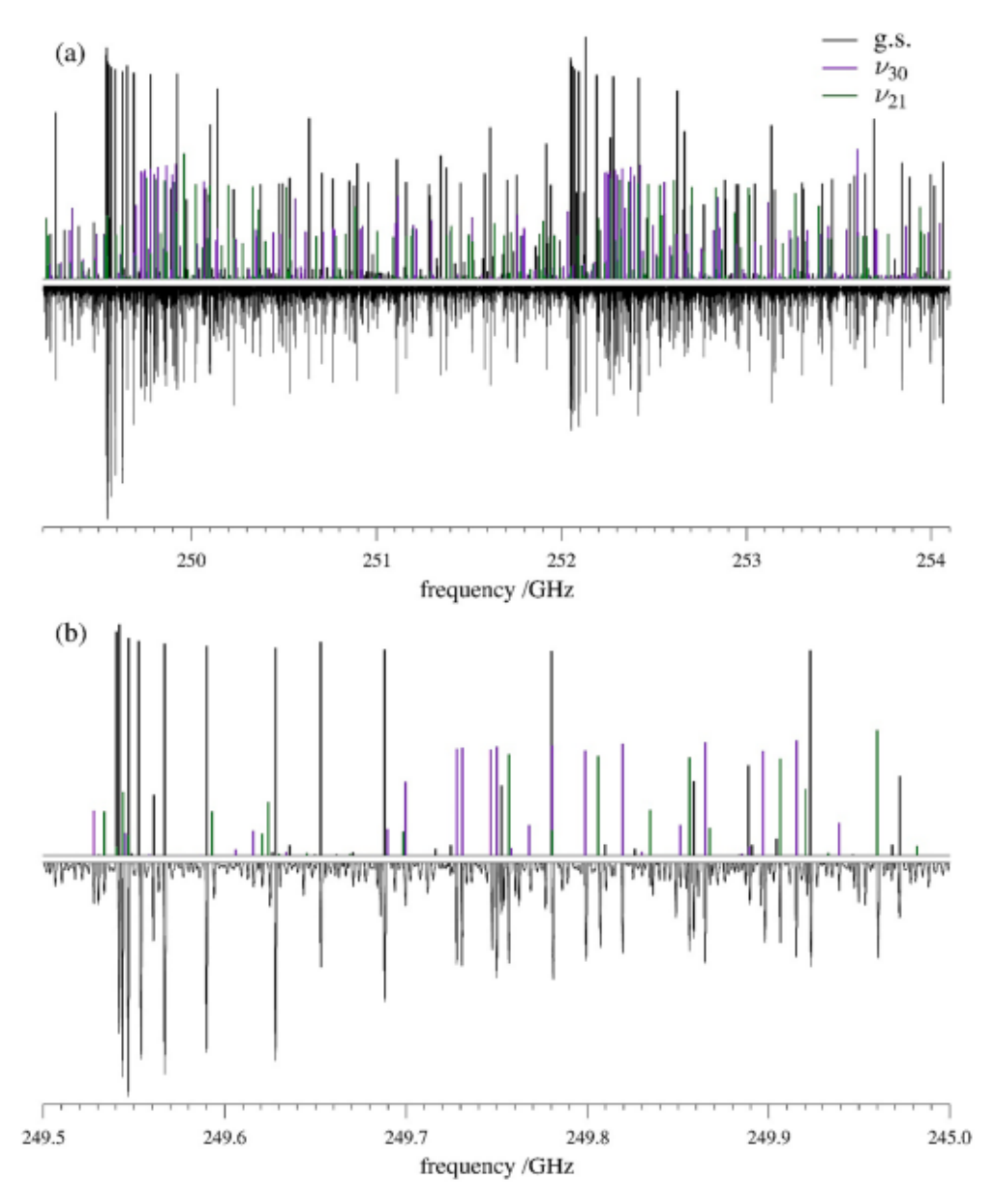


Fig. 3. (a) Experimental rotational spectrum (bottom) of 2-cyanopyridine from 249.2 to 254.1 GHz and predicted stick spectrum (top) from experimental spectroscopic constants. Prominent transitions of ground-state 2-cyanopyridine for the J'+1=99 and J'+1=100 bands appear in black. Transitions for ν_{30} are shown in purple, and transitions for ν_{21} are green. Unassigned transitions are attributable to other vibrationally excited states of 2-cyanopyridine. (b) Expansion showing experimental and predicted spectra near the J'+1=99 band region.

spectroscopic parameters, excluding the aforementioned h1 constant, are well predicted via the B3LYP/6-311+G(2d,p) calculation. The rotational constants have remarkably small differences between predicted and experimental values: 0.05% in A_0 , 0.11% in B_0 , and 0.08% in Co in both the A and S reductions. The computed quartic distortion constants are all within 14% of the experimental values, with the largest difference exhibited by Δ_{K} . Similarly, the sextic distortion constants are accurately predicted (within 23%), with the exceptions of Φ_J and h_1 (30% and 533%, respectively), suggesting that the experimental values are indeed physically meaningful. Excluding l_1 , all octic centrifugal distortion terms in the 8 reduction were well determined. In the A reduction, three on-diagonal octic terms were well-determined (L_{LIK} , L_{JK} , and L_{KKJ}), and the remaining terms were held constant at zero. No computational packages currently predict the octic centrifugal distortion terms to calibrate the meaningfulness of these values. Comparing experimental octic distortion constants for several analogous molecules,

however, will be discussed below.

3.2. Spectral analysis of v_{30} and v_{21}

Consistent with the 3- and 4-cyanopyridine regioisomers and other cyanoarenes [1–5,31,33], the two lowest-energy fundamental vibrational states of 2-cyanopyridine are in-plane (ν_{30} , A'', 154 cm⁻¹ [19]) and out-of-plane (ν_{21} , A', 175 cm⁻¹ [19]) bending modes of the CN group with respect to the pyridine ring. Initial predictions of the spectra of the vibrational excited states were made using the experimental ground-state rotational constants (as corrected using B3LYP-computed vibration-rotation interaction constants), in conjunction with experimental ground-state centrifugal distortion constants. In Fig. 6, the vibrational manifold of 2-cyanopyridine is shown up to 550 cm⁻¹ using fundamental vibrational energies observed by low-resolution Raman spectroscopy [19]. As expected, initial attempts to least-squares fit the

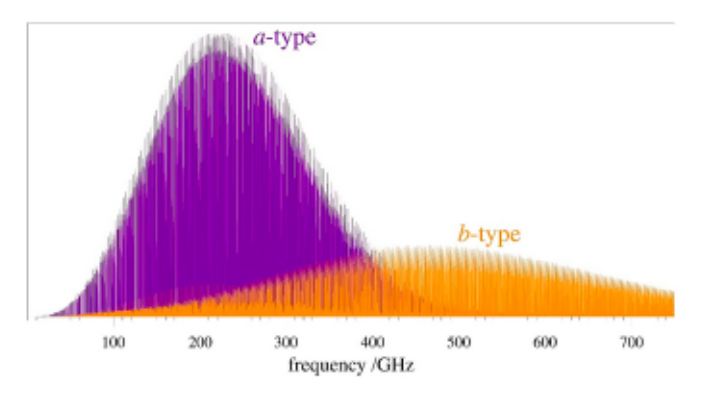


Fig. 4. Predicted rotational spectrum of the ground vibrational state of 2-cyanopyridine from experimental spectroscopic constants at 292 K (ambient temperature). a-Type transitions are displayed in purple, and b-type transitions are displayed in orange.

low- K_a series transitions of these vibrationally excited states to a single-state Hamiltonian were unsuccessful. The symmetries of ν_{30} and ν_{21} allow for a- and b-type Coriolis coupling interactions between these fundamental states. In order to account for the a-axis and b-axis Coriolis coupling, the two states were treated with a combined A-reduced Hamiltonian that included spectroscopic constants for each state, the energy separation $\Delta E_{30,21}$, initially set to the previously experimentally determined value [19], and computed Coriolis-coupling terms. As more perturbed transition frequencies were included in the data set, G_a and G_b terms were allowed to vary and additional higher-order coupling terms were added to model the rotational spectra of these two states. The A reduction was used to allow for comparison with previous studies of cyanoarenes and to maintain a consistent reduction with the common centrifugally distorted Coriolis terms, e.g., G_a^J , G_a^K , etc., which use an A-reduction centrifugal distortion expansion.

Fig. 3 shows the predicted and experimental spectra of 2-cyanopyridine in the ground state, ν_{30} , and ν_{21} , demonstrating the density of transitions within a 5 GHz section of the 600 GHz-wide spectral range studied in this work. In 2-cyanopyridine, Q-branch transitions were of sufficient intensity for a small set to be observed and measured in both excited states. Ultimately, over 6600 and 5800 transitions were measured for ν_{30} and ν_{21} , respectively, with J' values ranging from 11 to 198 and K_a'' values ranging from 0 to 57. The full range of Q- and R-branch transitions in ν_{30} and ν_{21} can be seen in the data distribution plots in Fig. 7. Although the breadth of data was lower for both excited states than for the ground state, the coverage proved nonetheless sufficient to obtain well-determined spectroscopic terms. The lack of high-error transitions in Fig. 7 indicates that the Hamiltonian was adequate to model the perturbed transition frequencies.

The spectroscopic constants for ν_{30} and ν_{21} (Table 2) are very similar in magnitude and sign as each of their respective ground-state constants - an indication that the constants have not absorbed a large amount of perturbation, which should ideally be addressed by coupling terms. Of the quartic distortion constants, the values of Δ_J and off-diagonal δ_J and δ_K are within 4% of the corresponding ground-state values, and the values of the sextic constants that could be determined $(\Phi_J, \phi_{JK}, \text{ and } \phi_{KJ})$ are within 14%. The values of these constants are shifted in the same direction relative to the ground state for each respective term, thus the changes of up to 14% are likely to be reasonable. The constants Δ_{JK} , Δ_{K} , and Φ_{KJ} have potentially absorbed coupling. For the Δ_{JK} and Φ_{KJ} values, the change in magnitudes are quite small (within 6.5% and 8.0% of the ground-state values, respectively), albeit in opposite directions for each pair of constants. For Δ_K , the change in magnitude is larger, with changes of -42.2% and +56.7% for the lower- and higher-energy states, respectively. This is slightly concerning, and it is possible that the Δ_K values have absorbed a small amount of the Coriolis coupling. Unfortunately, computational state-specific centrifugal distortion constants are not available to provide a meaningful estimate of the expected change in centrifugal distortion upon vibration. Nonetheless, the coupling is treated effectively, as evidenced by numerous, well-fit transitions affected by both global and local (resonances) perturbations, and we believe that the rotational and centrifugal distortion constants are largely free of Coriolis coupling, as demonstrated in Table 2.

Table 3 contains the computational and experimental vibration-rotation interaction constants (a_i values), energy separation,

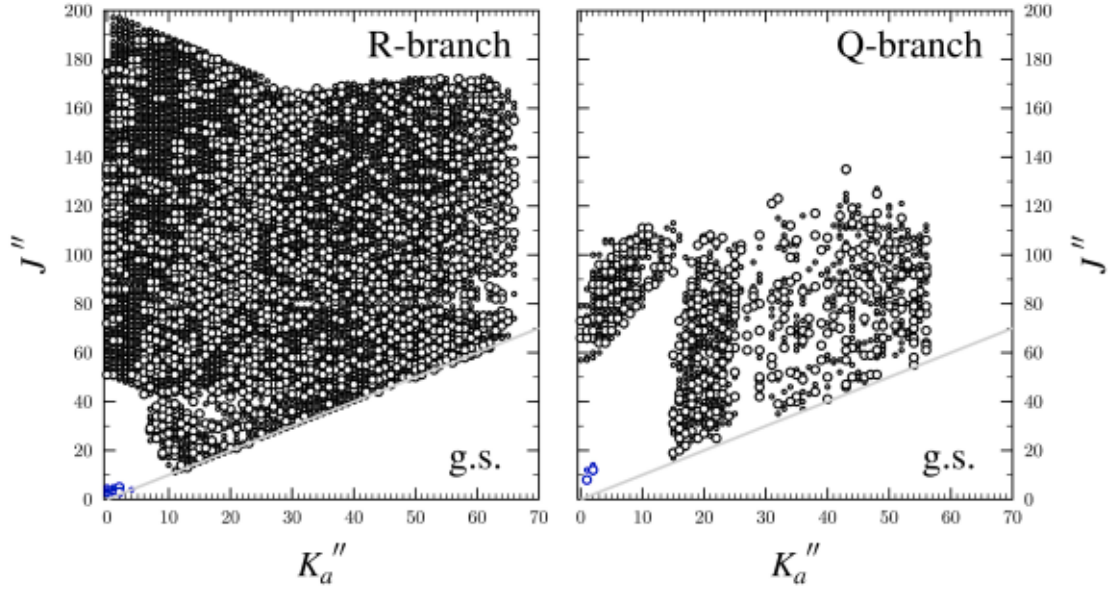


Fig. 5. Data distribution plots for the least-squares fit of spectroscopic data for the vibrational ground state of 2-cyanopyridine (A reduction, I^r representation). The size of the outlined circles in this plot corresponds to $|(f_{obs.} - f_{cutc.})/\delta f|$, where δf is the measurement uncertainty, and all quotient values are less than 3. Black symbols denote data from the present work, blue symbols denote data from Doraiswamy and Sharma [18].

Table 1

Experimental and computational spectroscopic constants for the ground vibrational state of 2-cyanopyridine (A- and S-reduced Hamiltonians, I' representation).

S reduction, I' representation			A reduction, I ^r representation			
	Current work	B3LYP ^a		Current work	B3LYP ^a	
A(5) (MHz)	5837.001016 (84)	5839.6	A(A) (MHz)	5837.000887 (83)	5839.6	
B(5) (MHz)	1598.232217 (16)	1596.4	$B_0^{(A)}$ (MHz)	1598.233457 (17)	1596.4	
C(S) (MH₂)	1254.458439 (17)	1253.4	C(A) (MH±)	1254.457178 (14)	1253.4	
D _j (kHz)	0.0349129 (15)	0.0338	Δ _J (kH ₂)	0.0473570 (11)	0.0455	
D _{JK} (kHz)	1.061181 (13)	0.999	Δ _{JK} (kHz)	0.986442 (12)	0.930	
D_K (kHz)	0.245618 (79)	0.279	$\Delta_K (kHz)$	0.307905 (71)	0.337	
d1 (kHz)	-0.01149063 (48)	-0.0110	δ _J (kHz)	0.01148853 (53)	0.0110	
d ₂ (kHz)	-0.00622494 (32)	-0.00578	δ _K (kHz)	0.638926 (27)	0.600	
H _J (Hz)	-0.000011785 (63)	-0.0000110	Φ _J (H ₂)	0.000003210 (26)	0.00000224	
H _{JK} (Hz)	0.00115935 (61)	0.000997	Φ_{JK} (Hz)	0.0016822 (32)	0.00144	
H _{KJ} (Hz)	-0.0063147 (71)	-0.00549	Φ_{KJ} (Hz)	-0.008322 (14)	-0.00717	
H_K (Hz)	0.006044 (30)	0.00510	Φ _K (Hz)	0.007526 (23)	0.00631	
h ₁ (Hz)	0.00000045 (12)	-0.00000195	ϕ_J (Hz)	0.000001390 (13)	0.00000107	
h ₂ (Hz)	0.000007666 (27)	0.0000663	φ _{JK} (Hz)	0.0008281 (19)	0.000730	
h ₃ (Hz)	0.000001511 (11)	0.00000126	φ _K (Hz)	0.008305 (57)	0.00703	
L _J (mHs)	0.0000001103 (92)		L _J (mHs)	[0.]		
Luk (mHz)	-0.000001974 (12)		L _{UK} (mHz)	-0.000002978 (91)		
L _{JK} (mHz)	0.00001876 (12)		L_{JK} (mHz)	-0.0000140 (16)		
L _{KK} (mHz)	-0.0001257 (14)		L_{KKJ} (mHz)	-0.0000208 (48)		
L _K (mHz)	0.0000741 (37)		L _K (mHz)	[0.]		
l ₁ (mHs)	[0.]		(mHz) را	[0.]		
l ₂ (mHs)	-0.0000000756 (54)		l _{JK} (mHz)	-0.000001175 (41)		
l ₃ (mHz)	-0.0000000295 (32)		l _{KJ} (mHz)	-0.0000115 (16)		
4 (mHs)	-0.00000000972 (86)		l _K (mHs)	-0.000342 (18)		
N _{lines} b	10,606°		N _{lines} b	10,606°		
σ _{fit} (MHz)	0.040		σ _{fit} (MHz)	0.040		
Δ_i (uÅ ²) ^d	0.073069 (6)		Δ_i (uÅ ²) d	0.073717 (6)		

^a Calculation at the B3LYP/6-311+G(2d,p) level.

^d Inertial defect ($\Delta_i = I_c - I_a - I_b$), calculated using PLANM.

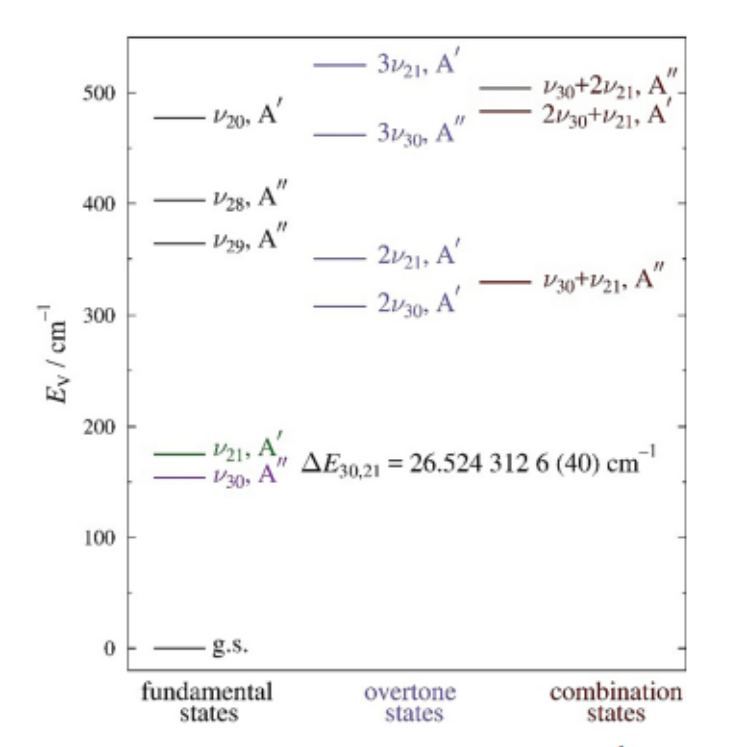


Fig. 6. Vibrational energy levels of 2-cyanopyridine below 550 cm⁻¹. Fundamental energies are experimental [19], while overtone and combination states are estimated. The value of $\Delta E_{30,21}$ results from the experimental perturbation analysis of ν_{30} and ν_{21} in this work.

Coriolis C constants, and averaged vibration-rotation interaction constants. The energy separation determined in this work is approximately 5 cm⁻¹ larger than that determined previously (21 cm⁻¹ [19]) but approximately 6 cm⁻¹ smaller than the B3LYP prediction. The computational over-prediction has been observed in previous investigations of monosubstituted aromatics [1,2,4,5,31-33]. The computed vibration-rotation interaction constants for Av, which correspond to the larger coupling term, show the telltale indication of Coriolis coupling, i. e., similarly large magnitudes (each over 100 MHz, in this case) of opposite sign. In contrast, the experimentally determined a_A values are rather small - varying by only single-MHz values - indicating that coupling has to a large extent been removed from these values. The averaged a_A value effectively cancels the Coriolis coupling effect found in the individual a_A values, and the agreement between computed and experimental values for this averaged value is exceptional. This is likely fortuitous in that the agreement is even better than those for the a_B and a_C averaged values. The a_B and a_C values, as well as their averaged values, demonstrate close agreement between theory and experiment. The inertial defects for these two vibrationally excited states change in the expected manner, increasing in absolute value relative to the ground state. The predicted ζ values are also in excellent agreement with those determined experimentally. Together, this level of agreement supports the notion that Coriolis coupling between the states has largely been addressed appropriately by the chosen Coriolis terms. The rotational and centrifugal distortion constants can be expected to be physically meaningful for these states.

b Number of independent transition frequencies.

^c Includes transitions from Doraiswamy and Sharma [18].

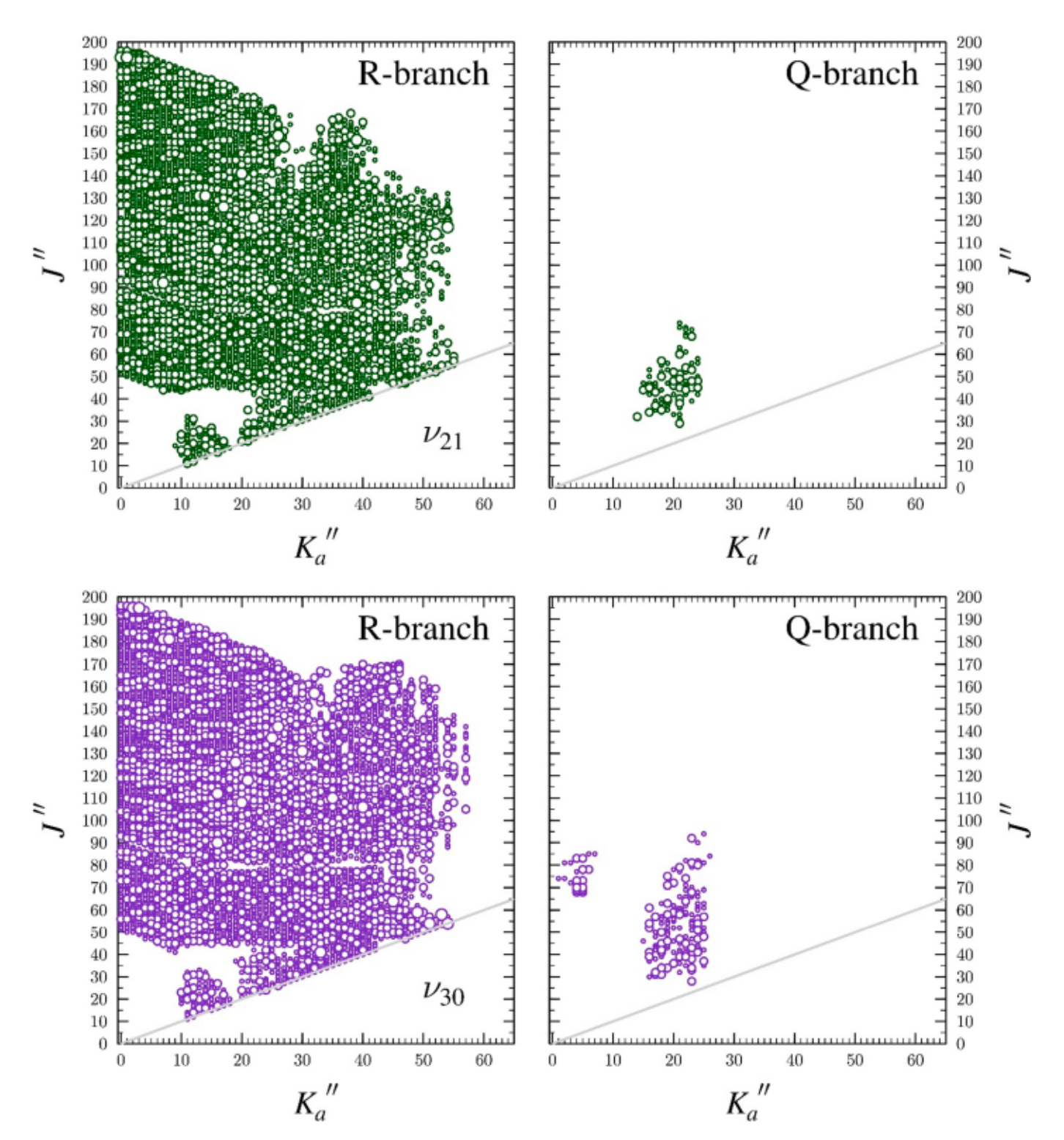


Fig. 7. Data distribution plots for the least-squares fit of spectroscopic data for the lowest-energy fundamental states of 2-cyanopyridine, ν_{30} (purple) and ν_{21} (green). The size of the outlined circles in this plot corresponds to $|(f_{obs.} - f_{calc.})/\delta f|$, where δf is the measurement uncertainty and all quotient values are less than 3.

Table 2Spectroscopic constants for the coupled dyad of 2-cyanopyridine (A-reduced Hamiltonian, I^r representation).

	Ground State	$_{30}$ (A , 154 cm $^{1})^{a,b}$	$_{21}$ (A , 175 cm 1) a,b
$A_{\nu}^{(A)}$ (MHz)	5837.000887 (83)	5838.259 (54)	5833.638 (54)
$B_{\nu}^{(A)}$ (MHz)	1598.233457 (17)	1600.017759 (18)	1601.240899 (20)
$C_{\nu}^{(A)}$ (MHz)	1254.457178 (14)	1256.400750 (19)	1255.331832 (22)
$_{J}$ (kHz)	0.0473570 (11)	0.04816617 (89)	0.04834711 (97)
$_{JK}$ (kHz)	0.986442 (12)	1.0273 (44)	0.9229 (44)
_K (kHz)	0.307905 (71)	0.17783 (100)	0.48236 (100)
$_{J}$ (kHz)	0.01148853 (53)	0.01156245 (22)	0.01186675 (29)
_K (kHz)	0.638926 (27)	0.639238 (23)	0.642574 (23)
$_{J}$ (Hz)	0.000003210 (26)	0.000003652 (16)	0.000003529 (18
$_{JK}$ (Hz)	0.0016822 (32)	0.0016733 (51)	0.0016713 (51)
_{KJ} (Hz)	0.008322 (14)	0.007659 (28)	0.008755 (29)
_K (Hz)	0.007526 (23)	[0.007526]	[0.007526]
$_{J}$ (Hz)	0.000001390 (13)	[0.00001390]	[0.00001390]
$_{JK}$ (Hz)	0.0008281 (19)	[0.0008281]	[0.0008281]
$_{K}$ (Hz)	0.008305 (57)	[0.008305]	[0.008305]
E _{30,21} (MHz)		795178.89 (12)	
$E_{30,21}$ (cm ¹)		26.5243126 (40)	
G_a (MHz)		9902.3 (22)	
G_a^J (MHz)		0.00613 (18)	
G_a^K (MHz)		0.004721 (45)	
G_a^{JJ} (MHz)		0.0000000260 (22)	
F_{bc} (MHz)		0.4308 (11)	
\mathcal{F}_{bc}^{J} (kHz)		0.000000509 (89)	
G_b (MHz)		48.426 (21)	
G_b^J (MHz)		0.0000753 (12)	
N _{lines} ^c	10,606	6603	5877
fit (MHz)	0.040	0.042	0.041
$_{i}$ (uÅ ²) ^{d}	0.073069 (6)	0.17820 (80)	0.33701 (80)

^a Condensed-phase fundamental frequencies from reference [19].

Table 3Experimental and computed vibration rotation interaction constants, Corioliscoupling constants, energy separation, and averaged vibration rotation interaction constants for excited vibrational states 30 and 21 of 2-cyanopyridine.

	Experimental	$B3LYP^a$	obs. calc.
A ₀ A ₃₀ (MHz)	1.258 (54)	105.5	106. 8
$B_0 = B_{30} \text{ (MHz)}$	1.78302 (25)	1.75	0.034
C_0 C_{30} (MHz)	1.94375 (24)	1.92	0.024
A_0 A_{21} (MHz)	3.363 (54)	103.4	106.7
$B_0 B_{21} \text{ (MHz)}$	3.007442 (26)	2.86	0.147
C_0 C_{21} (MHz)	0.874654 (26)	0.82	0.055
$\frac{A_0 A_{30} A_0 A_{21}}{2}$ (MHz)	1.052 (76)	1.05	0.002
$\frac{B_0 B_{30} B_{0} B_{21}}{2}$ (MHz)	2.395872 (36)	2.31	0.091
$\frac{C_0 C_{30} C_0 C_{21}}{2}$ (MHz)	1.409113 (35)	1.37	0.039
a 30 21	0.84824 (19)	0.819	0.021
b 30 21	0.0151499 (66)	0.0181	0.0075
$E_{30,21}$ (cm 1)	26.5243126 (40)	32.7	6.2

 $[^]a$ Evaluated with the 6-311 $\,$ G(2d,p) basis set.

4. Interpretation and analysis of resonances

The least-squares fit of the 2-cyanopyridine dyad includes several local resonances like those shown in Fig. 8, which involve pairs of rotational energy levels separated by K_a 4 between the two vibrational states. Fig. 9 demonstrates the progression of the undulations and

resonances present in $_{30}$. As visible in the plot, both the local resonances and undulations trend significantly larger as K_a increases, and the former are not noticeable at all in the lowest K_a series. The series that contain large resonances, e.g., K_a 14, are very important for good determination of the coupling terms and precise determination of the energy separation. As many of these resonances are found at frequencies beyond 410 GHz, spectral coverage up to 750 GHz was beneficial to achieve a thorough analysis of this dyad. Most of the transitions corresponding to the large local resonances shown in Fig. 9 (and in the interlacing odd K_a series, which are not explicitly shown in the figure, as well as those of $_{21}$) have been measured, assigned, and successfully incorporated into the regression analysis. On the other hand, we were not able to conclusively find or include any nominal interstate transitions, and indeed these are predicted to be rather weak for this dyad.

5. Discussion

The B3LYP/6 311 G(2d,p) predicted constants have proven to reliably estimate the rotational, quartic centrifugal distortion, and sextic centrifugal distortion constants of the ground vibrational state. Table 4 presents a comparison of the ground-state spectroscopic constants of the analogous molecules 2-cyanopyridine, 3-cyanopyridine [1], 4-cyanopyridine [2], 2-cyanopyrimidine [4], cyanopyrazine [5], and benzonitrile [32,33] to provide insight into the physical meaningfulness of these constants. As a consequence of the different frequency ranges over which these spectra were analyzed (2-cyanopyrimidine: 130 500 GHz, 2-cyanopyridine: 130 750 GHz, with relatively few measured transitions above 500 GHz, and the remaining molecules: 130 360 GHz), many of the spectroscopic constants of 2-cyanopyridine and 2-cyanopyrimidine are determined more precisely. The extensive frequency range

^b Bracketed values held constant at their respective ground-state value, all octic centrifugal distortion parameters (not shown) were held constant at their respective ground-state values.

^c Number of independent transition frequencies.

 $[^]d$ Inertial defect ($_i$ I_c I_a I_b) calculated from the B_v constants using PLANM.

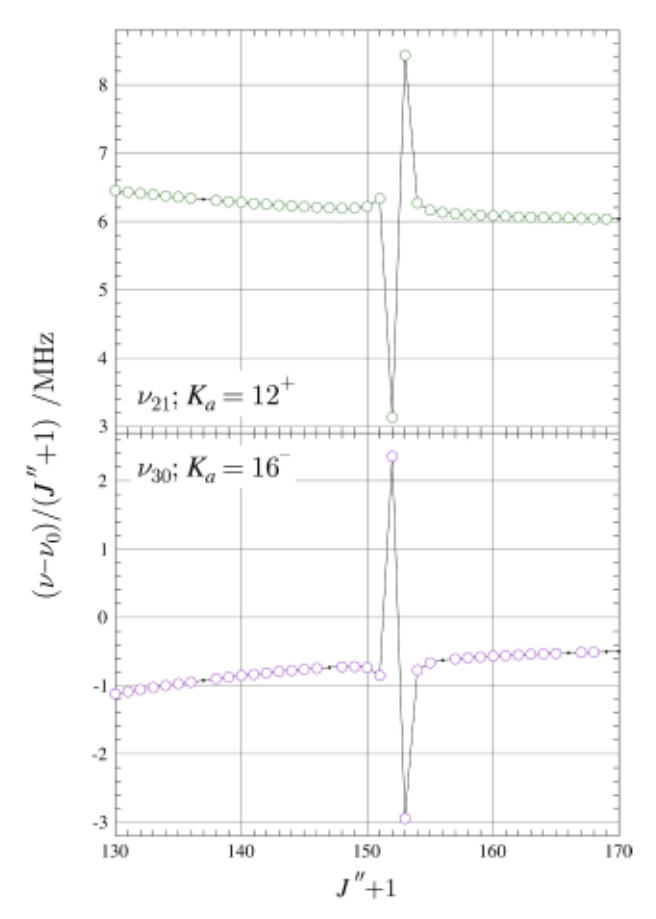


Fig. 8. Resonance plots for 2-cyanopyridine showing the $K_a=16^-$ series for ν_{30} and $K_a=12^+$ series for ν_{21} . This resonance conforms to the $\Delta K_a=4$ selection rule for a-type Coriolis interactions. The plotted values are frequency differences between excited-state transitions and their ground-state counterparts, scaled by (J'+1) in order to make the plots more horizontal. Measured transitions are represented by circles: ν_{30} (purple), ν_{21} (green). Predictions from the coupled least-squares fit are represented by a solid, colored line.

analyzed in both works, however, still does not provide enough information to determine a full set of octic terms. Only for 2-cyanopyridine could any off-diagonal octic constants be determined. With the exception of the 8-reduction least-squares fit of 2-cyanopyridine, at least one on-diagonal octic constant needed to be held at a value of zero for all of the cyanoarenes. The six molecules are structurally analogous, so the consistency in sign and order-of-magnitude across respective spectroscopic constants is expected, but nonetheless noteworthy. The signs and magnitudes are quite consistent across this set of molecules for any given constant. The largest and smallest rotational constants are within 7% of one another, the quartic centrifugal distortion constants are within 35%, and the sextic terms are within 37% (except Φ_J , whose smallest and largest values are within 53 %). Discrepancies in the octic centrifugal distortion terms are larger, as expected. In particular, the value of L_{JK} is quite consistent across all molecules for which it was determined except 2-cyanopyridine, where it is determined with the opposite sign (Table 4). This unique difference could indicate an error in the determination of this constant for 2-cyanopyridine. It is more likely, however, that the sign difference is due to the determination of off-diagonal octic centrifugal distortion terms for 2-cyanopyridine, and the lack thereof for any of the other molecules. Indeed, if the off-diagonal octic terms are held constant at values of zero, LJK becomes positive for 2-cyanopyridine, but numerous transitions have to be rejected, indicating the necessity of these terms in the least-squares fit. It is therefore possible that the sign discrepancy actually indicates that the L_{JK} values determined for the other four molecules are not physically meaningful.

Unfortunately, it would be necessary to determine the full set of octic centrifugal distortion constants in order to conclude which of the possibilities is the case. The only conclusion that can be drawn from the available data is that the distortion constants determined in any set, e.g., quartic, sextic, or octic, in which any constants are held to a value of zero should be considered somewhat empirical and not necessarily physically meaningful. Such a limitation provides further motivation for computational prediction of the octic centrifugal distortion constants.

The Coriolis-coupling terms of the analogous coupled dyads of 2-cyanopyridine, 3-cyanopyridine [1], 4-cyanopyridine [2], 2-cyanopyrimidine [4], cyanopyrazine [5], and benzonitrile [32,33], are compared in Table 5. It is important to note that only a-axis coupling exists for the dyads of benzonitrile, 4-cyanopyridine, and 2-cyanopyrimidine due to their molecular symmetry, i.e. $C_{2\nu}$, and they are grouped accordingly. Reasonably, the energy separations between the in-plane (ip) and out-ofplane (oop) nitrile bending modes vary across the different species, but the coupling terms show a fair degree of similarity. The dominant coupling term in these dyads, G_a , is ~10,000 MHz, while G_a^J is near -0.005 MHz and Fbc is approximately -0.4 MHz. These observations would seem to suggest that the determined values are physically meaningful. Within this group of molecules, there is some variation in the particular coupling terms that were able to be determined. For molecules in which like terms were determined, the signs of the determined values are largely consistent. The b-axis coupling terms show similar agreement across the investigated molecules.

6. Conclusion

The spectroscopic investigation of 2-evanopyridine presented in this work, combined with computational estimates of nuclear quadrupole coupling constants and previous experimental measurements of the other cyanopyridines, provide a sufficient basis for an astronomical search for the series of isomeric cyano-substituted pyridines [1,2,35]. The detection of pyridine, or any of its derivatives, in extraterrestrial environments would be a substantial breakthrough for the astrochemical community. The broad frequency coverage and large number of observed rotational transitions enables a determination of spectroscopic constants that are expected to predict transition frequencies very well to higher and lower frequencies. The ability to extrapolate to higher frequency arises, in part, due to the b-type transitions that dominate at higher frequency and share energy levels with a-type transitions included in the current data set. Not only was the broad frequency coverage helpful for analysis of the ground state, but it allowed for an excellent determination of the spectroscopic constants of the coupled dyad of vibrationally excited states ν_{30} and ν_{21} . A least-squares fit would have been possible from lower-frequency data, but the coupling was more precisely constrained by including the resonant transitions that occurred beyond 410 GHz.

Our recent work on the spectroscopy of cyano-arenes [1-5,32,33] provides motivation for the continued development of computational predictions of higher-order centrifugal distortion terms at the octic level. The very large data sets that include transitions at high J and K require many centrifugal distortion constants to achieve a low-error fit. With the incomplete determination of constants at this level, computed constants are needed to provide a reasonable benchmark and evidence that the experimental constants are likely to have physical meaning. Statespecific quartic centrifugal distortion constants have recently been determined for vibrationally excited states of the 1,2,3-triazoles [36] and had been determined previously for other smaller molecules. Despite these advances in predicting quartic centrifugal distortion constants, the inability to conveniently predict the quartic and sextic centrifugal distortion constants for vibrationally excited states limits the ability to assess the quality of the treatment of the Coriolis coupling in the vibrationally excited states. Additionally, a routine method has not been developed to predict higher-order Coriolis-coupling terms that

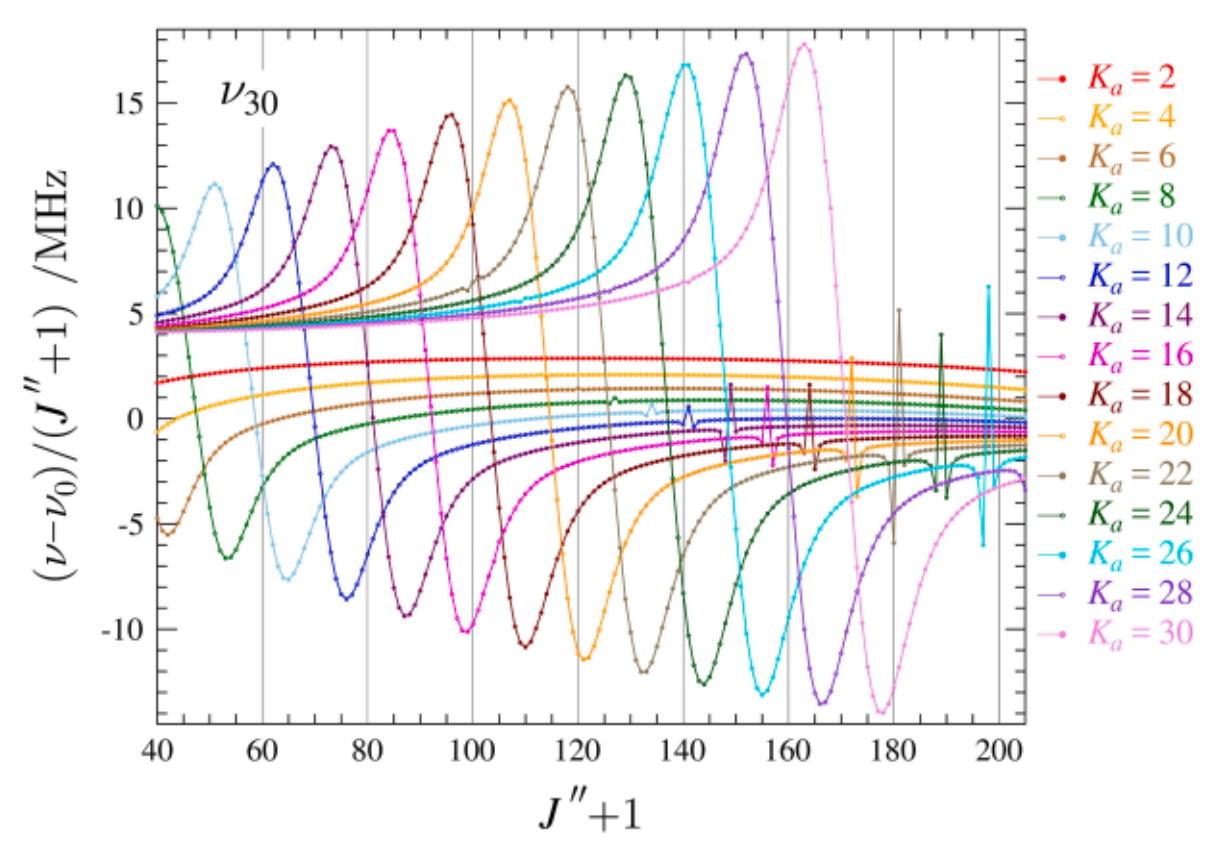


Fig. 9. Superimposed resonance plots of ν_{30} for ${}^{a}R_{0,1}$ even- K_{a}^{+} series from 2 to 30 for 2-cyanopyridine. Measured transitions are omitted for clarity, but they are indistinguishable from the plotted values on this scale. The plotted values are frequency differences between excited-state transitions and their ground-state counterparts, scaled by (J'' + 1).

Table 4

Spectroscopic constants for the ground vibrational states of 2-cyanopyridine, 3-cyanopyridine, 4-cyanopyridine, 2-cyanopyrimidine, cyanopyrazine, and benzonitrile (A-reduced Hamiltonian, I' representation).

	2-cyanopyridine	3-cyanopyridine [1]	4-cyanopyridine [2]	2-cyanopyrimidine [4]	cyanopyrazine [5]	benzonitrile [32]
A(A) (MHz)	5837.000887 (83)	5823.05832 (11)	6000.67028 (91)	6043.4539 (12)	6003.12822 (58)	5655.265428 (82)
B(A) (MHz)	1598.233457 (17)	1571.351896 (30)	1541.180078 (12)	1651.140609 (36)	1621.518806 (24)	1546.8757715 (80)
C(A) (MHz)	1254.457178 (14)	1237.169980 (23)	1225.999666 (11)	1296.639905 (39)	1276.427155 (25)	1214.4040832 (69)
Δ _J (kHs)	0.0473570 (11)	0.0464884 (30)	0.0469997 (26)	0.0483056 (22)	0.0492594 (19)	0.0452858 (14)
Δ _{JK} (kHz)	0.986442 (12)	1.063742 (28)	0.977719 (47)	1.037502 (25)	1.102415 (24)	0.937983 (20)
Δ _K (kHz)	0.307905 (71)	0.23366 (16)	0.3319 (27)	0.3608 (18)	0.3525 (13)	0.24411 (75)
δ _J (kHz)	0.01148853 (53)	0.0110955 (13)	0.01103714 (53)	0.01154427 (86)	0.01182909 (60)	0.01101116 (54)
δ _K (kHz)	0.638926 (27)	0.673712 (34)	0.64553 (17)	0.660687 (56)	0.702668 (42)	0.609187 (65)
Φ _J (Hz)	0.000003210 (26)	0.00000360 (12)	0.00000295 (11)	0.000001716 (84)	0.000001797 (74)	0.000002486 (60)
Φ _{JK} (Hz)	0.0016822 (32)	0.0018504 (47)	0.001718 (11)	0.0017323 (24)	0.0019713 (18)	0.0015586 (41)
Φ_{KJ} (Hz)	-0.008322 (14)	-0.009199 (21)	-0.009245 (47)	-0.008505 (15)	-0.009803 (15)	-0.007863 (16)
Φ_K (Hz)	0.007526 (23)	0.007488 (69)	[0.00708]	0.0107 (10)	0.01097 (83)	[0.0066915] ^a
φ _J (H ₂)	0.000001390 (13)	0.000001213 (58)	[0.00000116]	0.000001226 (19)	0.000001844 (15)	0.000001159 (26)
ϕ_{JK} (Hz)	0.0008281 (19)	0.0009081 (26)	0.0007997 (71)	0.0008021 (15)	0.0009204 (11)	0.0007398 (24)
φ _K (Hz)	0.008305 (57)	0.009045 (65)	0.00850 (22)	0.008258 (34)	0.009580 (31)	0.007480 (67)
L _J (mHs)	[0.]	[0.]	[0.]	0.000000167 (12)	0.000000361 (10)	[0.]
Luk (mHz)	-0.000002978 (91)	-0.00000242 (10)	-0.00000324 (12)	-0.000002409 (17)	-0.000002972 (15)	-0.000002198 (39)
Lux (mHz)	-0.0000140 (16)	0.00001754 (61)	0.00001391 (93)	0.00001448 (22)	0.00001795 (19)	[0.]
L _{KK} (mHz)	-0.0000208 (48)	-0.0001407 (34)	-0.0000991 (86)	-0.0001149 (31)	-0.0001153 (26)	-0.0000464 (18)
L _K (mHz)	[0.]	[0.]	[0.]	[0.]	[0.]	0.004501 (78)

^a Term held constant at the computationally predicted value.

Table 5
Energy separation between in-plane (ip) and out-of-plane (oop) nitrile bending modes and Coriolis-coupling coefficients for CN-substituted arenes.

	2-cyanopyridine C_s	3-cyanopyridine [1] C_s	cyanopyrazine [5] C_s	benzonitrile [32,33] $C_{2\nu}$	4-cyanopyridine [2] $C_{2\nu}$	2-cyanopyrimidine [4] $C_{2\nu}$
E _{ip oop} (cm ¹)	26.5243126 (40)	15.7524693 (37)	24.8245962 (60)	19.1081698 (67)	18.806554 (11)	38.9673191 (77)
G_a (MHz) G_a^I (MHz) G_a^K (MHz) G_a^K (MHz)	9902.3 (22) 0.00613 (18) 0.004721 (45) 0.00000000260 (22)	9708.1023 (44) 0.0050152 (79)	10789.33 (63) 0.0052515 (62) 0.029393 (77) 0.00000000517 (11)	9531. (46) 0.004594 (20)	10136.164 (24) 0.004687 (16)	10666.3 (75) 0.006165 (29) 0.00466 (14) 0.00000000635 (44)
G_a^{KK} (MHz)	0.00000000200 (22)		0.00000000017 (11)			0.00000000033 (44)
F_{bc} (MHz) F_{bc}^{J} (MHz)	0.4308 (11) 0.000000509 (89)	0.40297 (19)		0.412 (30)	0.41065 (31)	0.3779 (26)
F_{bc}^{K} (MHz)		0.00001113 (24)	0.00001287 (20)	0.00000896 (32)	0.00000784 (38)	0.000006992 (97)
G_b (MHz) G_b^I (MHz) G_b^K (MHz)	48.426 (21) 0.0000753 (12)	56.8014 (77) 0.00005652 (67) 0.000154 (18)	134.02 (45) 0.0000378 (12)			
F_{ac} (MHz) F_{ac}^{K} (MHz)			1.079 (12)			

include centrifugal distortion. Without computational predictions of higher-order coupling terms and centrifugal distortion constants for the vibrationally excited states, and considering the difficulty of acquiring a converging, low-error, least-squares fit that incorporates resonant transitions but minimizes absorption of perturbation into rotational and centrifugal distortion constants, it is difficult in reality, likely impossible to assess whether the values obtained from the least-squares fit are physically meaningful. At the present time, the spectroscopic constants that cannot be predicted have to be judged either by their ability to predict the perturbed rotational spectra or by comparison to analogous systems in similar molecules. This situation highlights the need for continued advances in computational predictions of spectroscopic constants.

Declaration of Competing Interest

The authors declare that they have no known competing financial interests or personal relationships that could have appeared to influence the work reported in this paper.

Data availability

The data are available in the manuscript and Supplementary Materials.

Acknowledgements

We gratefully acknowledge the National Science Foundation for support of this project (CHE-1664912 and CHE-1954270). P.M.D thanks the University of Wisconsin Madison Graduate School for support as an Advanced Opportunity Fellow.

Appendix A. Supplementary material

Supplementary material includes computational output files and least-squares fitting files of 2-cyanopyridine.

Supplementary data to this article can be found online at https://doi.org/10.1016/j,jms.2023.111842.

References

[1] P.M. Dorman, B.J. Esselman, R.C. Woods, R.J. McMahon, An analysis of the rotational ground state and lowest-energy vibrationally excited dyad of 3-cyanopyridine: Low symmetry reveals rich complexity of perturbations, couplings, and interstate transitions, J. Mol. Spectrosc. 373 (2020), 111373.

- [2] P.M. Dorman, B.J. Esselman, J.E. Park, R.C. Woods, R.J. McMahon, Millimeter-Wave Spectrum of 4-Cyanopyridine in its Ground State and Lowest-Energy Vibrationally Excited Dyad, 20 and 30, J. Mol. Spectrosc. 369 (2020), 111274.
- [3] B.J. Esselman, M.A. Zdanovskaia, W.H. Styers, A.N. Owen, S.M. Kougias, B. E. Billinghurst, J. Zhao, R.C. Woods, R.J. McMahon, Millimeter-Wave and High-Resolution Infrared Spectroscopy of 2-Furonitrile A Highly Polar Substituted Furan, J. Phys. Chem. A 127 (2023) 1909 1922.
- [4] H.H. Smith, B.J. Esselman, M.A. Zdanovskaia, R.C. Woods, R.J. McMahon, The 130 500 GHz rotational spectrum of 2-cyanopyrimidine, J. Mol. Spectrosc. 391 (2023), 111737.
- [5] B.J. Esselman, M.A. Zdanovskaia, H.H. Smith, R.C. Woods, R.J. McMahon, The 130 500 GHz rotational spectroscopy of cyanopyrazine (C₄H₃N₂-CN), J. Mol. Spectrosc, 389 (2022), 111703.
- [6] B.A. McGuire, A.M. Burkhardt, S.V. Kalenskii, C.N. Shingledecker, A.J. Remijan, E. Herbst, M.C. McCarthy, Detection of the Aromatic Molecule Benzonitrile (c-C₆H₅CN) in the Interstellar Medium, Science 359 (2018) 202 205.
- [7] M.L. Sita, P.B. Changala, C. Xue, A.M. Burkhardt, C.N. Shingledecker, K.L. Kelvin Lee, R.A. Loomis, E. Momjian, M.A. Siebert, D. Gupta, E. Herbst, A.J. Remijan, M. C. McCarthy, I.R. Cooke, B.A. McGuire, Discovery of Interstellar 2-Cyanoindene (2 C₉H₇CN) in GOTHAM Observations of TMC-1, Astrophys. J. Lett. 938 (2022) 1.12
- [8] B.A. McGuire, R.A. Loomis, A.M. Burkhardt, K.L.K. Lee, C.N. Shingledecker, S. B. Charnley, I.R. Cooke, M.A. Cordiner, E. Herbst, S. Kalenskii, M.A. Siebert, E. R. Willis, C. Xue, A.J. Remijan, M.C. McCarthy, Detection of two interstellar polycyclic aromatic hydrocarbons via spectral matched filtering, Science 371 (2021) 1265–1269.
- [9] J. Cernicharo, A.M. Heras, A.G.G.M. Tielens, J.R. Pardo, F. Herpin, M. Guélin, L.B. F.M. Waters, *Infrared Space Observatory s* Discovery of C₄H₂, C₆H₂, and Benzene in CRL 618, Astrophys. J. 546 (2001) L123.
- [10] S.B. Charnley, Y.-J. Kuan, H.-C. Huang, O. Botta, H.M. Butner, N. Cox, D. Despois, P. Ehrenfreund, Z. Kisiel, Y.-Y. Lee, A.J. Markwick, Z. Peeters, S.D. Rodgers, Astronomical searches for nitrogen heterocycles, Adv. Space Res. 36 (2005) 137–145.
- [11] T.J. Barnum, M.A. Siebert, K.L.K. Lee, R.A. Loomis, P.B. Changala, S.B. Charnley, M.L. Sita, C. Xue, A.J. Remijan, A.M. Burkhardt, B.A. McGuire, I.R. Cooke, A Search for Heterocycles in GOTHAM Observations of TMC-1, J. Phys. Chem. A 126 (2022) 2716–2728.
- [12] R. Batchelor, J. Brooks, P. Godfrey, R. Brown, A Search for Interstellar Molecular Lines in the Frequency Range 8 6 to 9 2 GHz, Aust. J. Phys. 26 (1973) 557 560.
- [13] M.N. Simon, M. Simon, Search for Interstellar Acrylonitrile, Pyrimidine, and Pyridine, Astrophys. J. 184 (1973) 757 762.
- [14] R.G. Ford, The microwave spectra and dipole moments of the cyanopyridines, J. Mol. Spectrosc. 58 (1975) 178 184.
- [15] N. Vogt, L.S. Khaikin, A.N. Rykov, O.E. Grikina, A.A. Batiukov, J. Vogt, I. V. Kochikov, I.F. Shishkov, The equilibrium molecular structure of 2-cyanopyridine from combined analysis of gas-phase electron diffraction and microwave data and results of ab initio calculations, Struct. Chem. 30 (2019) 1699 1706.
- [16] L.S. Khaikin, N. Vogt, A.N. Rykov, O.E. Grikina, J. Demaison, J. Vogt, I. V. Kochikov, Y.D. Shishova, E.S. Ageeva, I.F. Shishkov, The Equilibrium Molecular Structure of 4-Cyanopyridine According to a Combined Analysis of Gas-Phase Electron Diffraction and Microwave Data and Coupled-Cluster Computations, Russ. J. Phys. Chem. A 92 (2018) 1970 1974.
- [17] L.S. Khaikin, N. Vogt, A.N. Rykov, O.E. Grikina, J. Vogt, I.V. Kochikov, E.S. Ageeva, I.F. Shishkov, The equilibrium molecular structure of 3-cyanopyridine according to gas-phase electron diffraction and microwave data and the results of quantum-chemical calculations, Mendeleev Commun. 28 (2018) 236–238.
- [18] S. Doraiswamy, S.D. Sharma, Microwave spectrum of 2-cyanopyridine, Curr. Sci. 40 (1971) 398 399.

- [19] J.H.S. Green, D.J. Harrison, Vibrational spectra of cyano-, formyl- and halogenopyridines, Spectrochim. Acta A 33 (1977) 75-79.
- [20] B.K. Amberger, B.J. Esselman, J.F. Stanton, R.C. Woods, R.J. McMahon, Precise equilibrium structure determination of hydrazoic acid (HN₃) by millimeter-wave spectroscopy, J. Chem. Phys. 143 (2015), 104310.
- [21] B.J. Esselman, B.K. Amberger, J.D. Shutter, M.A. Daane, J.F. Stanton, R.C. Woods, R.J. McMahon, Rotational Spectroscopy of Pyridazine and its Isotopologs from 235 360 GHz: Equilibrium Structure and Vibrational Satellites, J. Chem. Phys. 139 (2013), 224304.
- [22] H.H. Smith, B.J. Esselman, S.A. Wood, J.F. Stanton, R.C. Woods, R.J. McMahon, Improved semi-experimental equilibrium structure and high-level theoretical structures of ketene, J. Chem. Phys. 158 (2023), 244304.
- [23] Z. Kisiel, L. Pszczó kowski, I.R. Medvedev, M. Winnewisser, F.C. De Lucia, E. Herbst, Rotational Spectrum of trans trans Diethyl Ether in the Ground and Three Excited Vibrational States, J. Mol. Spectrosc. 233 (2005) 231 243.
- [24] Z. Kisiel, M.-A. Martin-Drumel, O. Pirali, Lowest vibrational states of acrylonitrile from microwave and synchrotron radiation spectra, J. Mol. Spectrosc. 315 (2015) 83, 01
- [25] H.M. Pickett, Determination of collisional linewidths and shifts by a convolution method, Appl. Opt. 19 (1980) 2745–2749.
- [26] H.M. Pickett, The fitting and prediction of vibration-rotation spectra with spin interactions, J. Mol. Spectrosc. 148 (1991) 371–377.
- [27] Z. Kisiel, Assignment and Analysis of Complex Rotational Spectra, in: J. Demaison, K. Sarka, E.A. Cohen (Eds.), Spectroscopy from Space, Springer, Netherlands, Dordrecht, 2001, pp. 91 106.
- [28] Z. Kisiel, PROSPE-Programs for ROtational SPEctroscopy. http://info.ifpan.edu.pl/~kisiel/prospe.htm.
- [29] J.R. Schmidt, W.F. Polik, WebMO Enterprise. 17.0.012e ed.; WebMO, LLC., Holland, MI, USA, 2017.
- [30] M.J. Frisch, G.W. Trucks, H.B. Schlegel, G.E. Scuseria, M.A. Robb, J.R. Cheeseman, G. Scalmani, V. Barone, G.A. Petersson, H. Nakatsuji, X. Li, M. Caricato, A.V. Marenich, J. Bloino, B.G. Janesko, R. Gomperts, B. Mennucci, H.P. Hratchian, J.V.

- Ortiz, A.F. Izmaylov, J.L. Sonnenberg, D. Williams-Young, F. Ding, F. Lipparini, F. Egidi, J. Goings, B. Peng, A. Petrone, T. Henderson, D. Ranasinghe, V.G. Zakrzewski, J. Gao, N. Rega, G. Zheng, W. Liang, M. Hada, M. Ehara, K. Toyota, R. Fukuda, J. Hasegawa, M. Ishida, T. Nakajima, Y. Honda, O. Kitao, H. Nakai, T. Vreven, K. Throssell, J.A. Montgomery, Jr., J.E. Peralta, F. Ogliaro, M.J. Bearpark, J.J. Heyd, E.N. Brothers, K.N. Kudin, V.N. Staroverov, T.A. Keith, R. Kobayashi, J. Normand, K. Raghavachari, A.P. Rendell, J.C. Burant, S.S. Iyengar, J. Tomasi, M. Cossi, J.M. Millam, M. Klene, C. Adamo, R. Cammi, J.W. Ochterski, R.L. Martin, K. Morokuma, O. Farkas, J.B. Foresman, D.J. Fox, Gaussian 16 rev C.01. Gaussian, Inc., Wallingford, CT, USA, 2016.
- [31] M.A. Zdanovskaia, B.J. Esselman, R.C. Woods, R.J. McMahon, The 130 370 GHz rotational spectrum of phenyl isocyanide (C₆H₅NC), J. Chem. Phys. 151 (2019), 024301.
- [32] M.A. Zdanovskaia, M.-A. Martin-Drumel, Z. Kisiel, O. Pirali, B.J. Esselman, R. C. Woods, R.J. McMahon, The eight lowest-energy vibrational states of benzonitrile: analysis of Coriolis and Darling-Dennison couplings by millimeter-wave and far-infrared spectroscopy, J. Mol. Spectrosc. 383 (2022), 111568.
- [33] M.A. Zdanovskaia, B.J. Esselman, H.S. Lau, D.M. Bates, R.C. Woods, R.J. McMahon, Z. Kisiel, The 103 360 GHz Rotational Spectrum of Benzonitrile, the First Interstellar Benzene Derivative Detected by Radioastronomy, J. Mol. Spectrosc. 351 (2018) 39 48.
- [34] Z. Kisiel, A. Kraśnicki, The millimetre-wave rotational spectrum of phenylacetylene, J. Mol. Spectrosc. 262 (2010) 82–88.
- [35] N. Vogt, K.P.R. Nair, J.-U. Grabow, J. Demaison, Microwave rotational spectrum and ab initio computations on 4-cyanopyridine: molecular structure and hyperfine interactions, Mol. Phys. 116 (2018) 3530–3537.
- [36] M.A. Zdanovskaia, P.R. Franke, B.J. Esselman, B.E. Billinghurst, J. Zhao, J. F. Stanton, R.C. Woods, R.J. McMahon, Vibrationally excited states of 1H- and 2H 1,2,3-triazole isotopologues analyzed by millimeter-wave and high-resolution infrared spectroscopy with approximate state-specific quartic distortion constants, J. Chem. Phys. 158 (2023), 044301.